THE JOURNAL OF BIOLOGICAL CHEMISTRY VOL. 281, NO. 8, pp. 4708–4717, February 24, 2006

Inhibition of RecA Protein Function by the RdgC Protein from *Escherichia coli*[*] [S]

Received for publication, December 21, 2005 Published, JBC Papers in Press, December 22, 2005, DOI 10.1074/jbc.M513592200

Julia C. Drees, Sindhu Chitteni-Pattu, Darrell R. McCaslin, Ross B. Inman, and Michael M. Cox[1]

From the Department of Biochemistry, University of Wisconsin, Madison, Wisconsin 53706-1544

The *Escherichia coli* RdgC protein is a potential negative regulator of RecA function. RdgC inhibits RecA protein-promoted DNA strand exchange, ATPase activity, and RecA-dependent LexA cleavage. The primary mechanism of RdgC inhibition appears to involve a simple competition for DNA binding sites, especially on duplex DNA. The capacity of RecA to compete with RdgC is improved by the DinI protein. RdgC protein can inhibit DNA strand exchange catalyzed by RecA nucleoprotein filaments formed on single-stranded DNA by binding to the homologous duplex DNA and thereby blocking access to that DNA by the RecA nucleoprotein filaments. RdgC protein binds to single-stranded and double-stranded DNA, and the protein can be visualized on DNA using electron microscopy. RdgC protein exists in solution as a mixture of oligomeric states in equilibrium, most likely as monomers, dimers, and tetramers. This concentration-dependent change of state appears to affect its mode of binding to DNA and its capacity to inhibit RecA. The various species differ in their capacity to inhibit RecA function.

Homologous recombination systems provide an essential avenue for the repair of stalled replication forks and contribute in other ways to the maintenance of genome integrity (1–6). RecA protein is a key component of recombinational DNA repair systems in bacteria. RecA functions in the form of nucleoprotein filaments that are assembled most readily on single-stranded DNA (ssDNA).[2] Filament assembly on duplex DNA (dsDNA) can also be achieved under some conditions, especially if a suitable nucleation site is available. RecA is a DNA-dependent ATPase, promoting ATP hydrolysis with a k_{cat} of ~30 or 20 min^{-1} when bound to ssDNA or dsDNA, respectively. RecA filaments assemble and disassemble in the 5′ to 3′ direction on ssDNA, with protomers being added to one end and subtracted from the other under appropriate conditions (7–10).

The activities of RecA protein must be regulated in the cell to target RecA to locations where it is needed and to avoid aberrant DNA transactions. This is true of all RecA homologs in all classes of organisms. The aberrant reactions could in principle include gross chromosomal rearrangements that lead to many human diseases, including cancer (11). Understanding how the RecA family of recombinases are regulated is thus of utmost importance.

RecA itself provides one level of control. This involves autoregulation mediated by the RecA C terminus (12–14). In *Escherichia coli*, many additional proteins are known to regulate RecA function. The RecF, RecO, and RecR proteins have been implicated in the modulation of RecA filament assembly (8, 15–17). The DinI protein is a generally positive modulator of RecA function during the SOS response (18–22), acting to stabilize RecA filaments (22). The RecX protein is an inhibitor of RecA function both *in vivo* and *in vitro* (23–25).

The *E. coli* RdgC protein may also regulate RecA function, directly or indirectly. The *rdgC* gene appears to be restricted to the Beta and Gamma subdivisions of the proteobacteria (26). During exponential growth, there are ~1000 dimers of RdgC protein present per cell (26), so the cellular concentration is similar to that of the *E. coli* SSB protein. Deletion of the *rdgC* gene in nuclease-deficient *recBC sbcBC* mutant strains is only possible if the RecA and RecF proteins are functional (hence, recombination-dependent growth) (27). The RdgC protein is also important in strains lacking PriA, the replication restart protein, because it alleviates a toxic effect of the RecFOR proteins (26). Mutations in SSB also alleviate this toxic effect (26). Because RecFOR are implicated in loading RecA onto SSB-coated DNA, the toxic effect could be due to formation of RecA filaments at inappropriate times or places (26). It is possible that RdgC, like SSB, binds to DNA to prevent RecA filament formation. *In vitro*, RdgC has been shown to bind both double-stranded and single-stranded DNA, with stronger binding to the duplex DNA (26). The results suggest a role for RdgC protein at stalled replication forks. RdgC might interact with RecA, SSB, or any of the other proteins that regulate RecA (RecF, RecO, RecR, DinI, or RecX). To begin an *in vitro* exploration of the function of RdgC protein, we here investigate the effects of RdgC on RecA function.

EXPERIMENTAL PROCEDURES

Enzymes—The *E. coli* wild-type RecA protein and the RecAΔC17 mutant were purified as described previously (13). The concentrations of the purified proteins were determined from the absorbance at 280 nm using the extinction coefficient $2.23 \times 10^4\ M^{-1}\ cm^{-1}$ (28). The *E. coli* SSB protein was purified as described before (29). The concentration of the purified protein was determined from the absorbance at 280 nm using the extinction coefficient $2.83 \times 10^4\ M^{-1}\ cm^{-1}$ (30).

Buffers, Media, and Reagents—R buffer contained 20 mM Tris-HCl (80% cation, pH 7.5), 1 mM DTT, 0.1 mM EDTA, and 10% (w/v) glycerol. TAE buffer contained 40 mM Tris-OAc (80% cation) and 1 mM EDTA. Luria-Bertani medium (LB broth) is 10 g/liter Tryptone, 5 g/liter yeast extract, and 10 g/liter NaCl, with pH adjusted to 7.0. Laemmli sample buffer contained 250 mM Tris-Cl, pH 6.8, 4% SDS, 20% (w/v) glycerol, 10% β-MeOH, and 0.1% (w/v) bromphenol blue. TBE buffer contained 90 mM Tris borate and 10 mM EDTA. Fluorescence polarization buffer contained 25 mM Tris-OAc (80% cation), 5% (w/v) glycerol, 3 mM potassium glutamate, 10 mM $Mg(OAc)_2$, 0.1 mM EDTA, 0.1 mg/ml bovine serum albumin, and 1 mM DTT.

* This work was supported by Grant GM52725 from the National Institutes of General Medical Sciences (to M. M. C. and R. B. I.). The costs of publication of this article were defrayed in part by the payment of page charges. This article must therefore be hereby marked "*advertisement*" in accordance with 18 U.S.C. Section 1734 solely to indicate this fact.

[S] The on-line version of this article (available at http://www.jbc.org) contains supplemental text and references.

[1] To whom correspondence should be addressed: Dept. of Biochemistry, University of Wisconsin-Madison, 433 Babcock Drive, Madison, WI 53706-1544. Tel.: 608-262-1181; Fax: 608-265-2603; E-mail: cox@biochem.wisc.edu.

[2] The abbreviations used are: ssDNA, single-stranded DNA; dsDNA, double-stranded DNA; ldsDNA, linear double-stranded DNA; cssDNA, circular single-stranded DNA; DTT, dithiothreitol.

Unless otherwise noted, all reagents were purchased from Fisher and were of the highest grade available. XhoI restriction endonuclease was purchased from MBI Fermentas. DTT was obtained from Research Organics. Lysozyme, phosphoenolpyruvate, pyruvate kinase, ATP, polyethyleneimine, bromphenol blue, phosphocreatine, and NADH were purchased from Sigma. Isopropyl-1-thio-β-D-galactopyranoside was obtained from Gold Bio Technology, Inc. Creatine phosphokinase was purchased from Roche Molecular Biochemicals. Ficoll was from Amersham Biosciences. Bovine serum albumin was from Promega.

Cloning and Overexpressing the RdgC Protein—Competent cells of *E. coli* strain STL327/pT7pol26 (13, 31) were transformed with plasmid pEAW379 carrying the *rdgC* gene under the control of the T7 RNA polymerase promoter. 10 liters of culture was grown in LB broth to 0.64 at A_{600}. RdgC protein expression was induced by the addition of isopropyl-1-thio-β-D-galactopyranoside to 0.2 mM. Following a 4-h incubation at 37 °C, 12.7 g of cells was harvested by centrifugation, flash-frozen in liquid N_2, and stored at −80 °C. The protein expressed is the native polypeptide, with no protein tags or other additions present.

Purification of the RdgC Protein—All steps were carried out at 4 °C. Cell paste (12.7 g) was thawed and fully resuspended in 80 ml of 25% (w/v) sucrose and 250 mM Tris-HCl (80% cation, pH 7.5). Cells were lysed by a 60-min incubation with 40 ml of 5 mg/ml solution of lysozyme in 250 mM Tris-HCl (80% cation, pH 7.5), followed by the addition of 50 ml of 25 mM EDTA, sonication, and centrifugation. The cleared lysate was fractionated with 35–70% ammonium sulfate. The RdgC protein was collected from the final cut by centrifugation. The pellet was resuspended in R buffer plus 1.5 M ammonium sulfate (5 ml per g of cell paste) and loaded onto a butyl-Sepharose column. The column was washed with R buffer plus 1.5 M ammonium sulfate. RdgC was eluted with a linear gradient from R buffer plus 1.5 M ammonium sulfate to R buffer over 10 column volumes. Peak fractions were identified by SDS-PAGE analysis, pooled, and dialyzed *versus* R buffer plus 50 mM KCl. RdgC was loaded onto a Source 15Q column equilibrated with R buffer plus 50 mM KCl and washed with the same buffer. RdgC was eluted with a linear gradient from R buffer plus 50 mM KCl to R buffer plus 500 mM KCl over 10 column volumes. Peak fractions were identified by SDS-PAGE analysis, tested individually for nuclease contamination, then pooled and dialyzed into R buffer plus 50 mM potassium acetate. The RdgC protein preparation used in this study was over 98% homogeneous and free of detectable nucleases. The concentration of the purified RdgC protein was determined from the absorbance at 280 nm using an extinction coefficient for RdgC, $\epsilon = 2.98 \times 10^4 \pm 0.15\ \mathrm{M}^{-1}\ \mathrm{cm}^{-1}$. This extinction coefficient was determined during the present study using a modification of a published procedure (32), described in detail in the online supplementary material.

DNA Substrates—Bacteriophage φX174 circular single-stranded DNA (virion) was purchased from New England Biolabs. φX174 RF I supercoiled circular duplex DNA was purchased from Invitrogen. Full-length linear duplex DNA was generated by the digestion of φX174 RF I DNA (5386 bp) with the XhoI restriction endonuclease, using conditions suggested by the enzyme supplier. The digested DNA was extracted with phenol/chloroform/isoamyl alcohol (25:24:1), followed by ethanol precipitation. Circular single-stranded DNA from bacteriophage M13mp8 (7229 nucleotides) was prepared using previously described methods (33). The fluorescently labeled oligonucleotide was purchased from Integrated DNA Technologies, Inc. Poly(dT) was purchased from Amersham Biosciences. The concentrations of ssDNA and dsDNA were determined by absorbance at 260 nm, using 36 and 50 μg ml^{-1} $A_{260}{}^{-1}$, respectively, as conversion factors. All DNA concentrations are given in micromolar nucleotides except where noted.

ATPase Assay—A coupled spectrophotometric enzyme assay (10, 34) was used to measure the DNA-dependent ATPase activities of the RecA protein. The regeneration of ATP from phosphoenolpyruvate and ADP was coupled to the oxidation of NADH and followed by the decrease in absorbance of NADH at 380 nm (380 nm wavelength was used so that the signal remained within the linear range of the spectrophotometer for the duration of the experiment). The assays were carried out on a Varian Cary 300 dual beam spectrophotometer equipped with a temperature controller and a 12-position cell changer. The cell path length and band pass were 1 cm and 2 nm, respectively. The NADH extinction coefficient at 380 nm of 1.21 $\mathrm{mM}^{-1}\ \mathrm{cm}^{-1}$ was used to calculate the rate of ATP hydrolysis.

The reactions were carried out at 37 °C in 25 mM Tris-OAc (80% cation, pH 7.4), 1 mM DTT, 3 mM potassium glutamate, 10 mM $Mg(OAc)_2$, 5% (w/v) glycerol, an ATP regeneration system (10 units/ml pyruvate kinase and 3.5 mM phosphoenolpyruvate), a coupling system (1.5 mM NADH and 10 units/ml lactate dehydrogenase), and 4 μM M13mp8 circular single-stranded DNA. The aforementioned components were incubated for 10 min. The figure legends note the time of addition of wild-type RecA protein (usually 2.4 μM), the RdgC protein (concentration indicated in the figure legends), the SSB protein (0.4 μM when present), and ATP (3 mM).

DNA Three-strand Exchange Reactions Promoted by the RecA Protein—Three-strand exchange reactions were carried out in 25 mM Tris-OAc (80% cation, pH 7.4), 1 mM DTT, 5% (w/v) glycerol, 3 mM potassium glutamate, 10 mM $Mg(OAc)_2$, and an ATP regeneration system (10 units/ml creatine phosphokinase and 12 mM phosphocreatine). All incubations were carried out at 37 °C. The following are final concentrations. The wild-type RecA protein, 3 μM, and 21 μM DinI protein (when included) were preincubated with 9 μM φX174 circular ssDNA for 5 min. SSB protein (0.9 μM) and ATP (3 mM) were then added, followed by another 5-min incubation. The reactions were initiated by the addition of φX174 linear dsDNA to 9 μM and after 5-min of incubation, the indicated concentration of RdgC protein was added. The reactions were incubated for 60 min. To stop the reaction, a 10-μl aliquot was removed and added to 5 μl of a solution containing 15% Ficoll, 4% SDS, 0.24% Bromphenol Blue, 0.24% xylene cyanol, and 72 mM EDTA. Samples were subjected to electrophoresis in 0.8% agarose gels with 1× TAE buffer, stained with ethidium bromide, and exposed to ultraviolet light. Gel images were captured with a digital charge-coupled device camera utilizing GelExpert software (Nucleotech).

RecA-promoted LexA Cleavage Assay—Reactions were carried out in 25 mM Tris-OAc (80% cation, pH 7.4), 1 mM DTT, 5% (w/v) glycerol, 3 mM potassium glutamate, 3 mM $Mg(OAc)_2$, and an ATP-regeneration system (2 mM phosphoenolpyruvate and 10 units/ml pyruvate kinase). The following are final concentrations. All incubations were at 37 °C. The reactions contained wild-type RecA protein (3 μM), φX174 circular ssDNA (9 μM), the SSB protein (0.9 μM, where indicated), ATP (3 mM), and RdgC (concentrations indicated in figure legend). The order of addition varies and is described in the figure legends. The LexA protein (3 μM) was added to start the reaction. All reactions were incubated for 15 min. Laemmli sample buffer (5 μl) was added to 10-μl reactions to stop the reaction. Samples were subjected to SDS-PAGE electrophoresis on 17% acrylamide gels and stained with Coomassie Brilliant Blue.

Electrophoretic Mobility Shift Assays—A fluorescently end-labeled single-stranded 30-mer oligonucleotide was purchased and used in these experiments. For one experiment, the labeled DNA was annealed to a complementary unlabeled 30-mer complement to produce a 30-bp blunt duplex oligonucleotide. The annealing reaction contained 1 μM

molecules each of labeled and unlabeled DNA, 25 mM Tris-OAc (80% cation, pH 7.4), 5% (w/v) glycerol, 3 mM potassium glutamate, and 10 mM $Mg(OAc)_2$ and was placed in a boiling water bath and allowed to cool. The labeled DNA was used at 10 nM in molecules in DNA binding reactions containing 25 mM Tris-OAc (80% cation, pH 7.4), 1 mM DTT, 3 mM potassium glutamate, 10 mM $Mg(OAc)_2$, and 5% (w/v) glycerol. These components were incubated at 37 °C with varying concentrations of RdgC protein or RdgC storage buffer. After 10 min, 10 μl of each reaction was added to 5 μl of loading dye (20% Ficoll and 20 mM Tris-OAc 80% cation), and the reactions were loaded onto a native 10% polyacrylamide gel and subjected to electrophoresis in TBE buffer. Results were read using a Typhoon 9410 Variable Mode Imager by Amersham Biosciences.

Sedimentation Equilibrium—To prepare samples for sedimentation equilibrium, an aliquot of RdgC protein was dialyzed at 4 °C into 20 mM Tris-HCl (80% cation, pH 7.5), 0.1 mM EDTA, and 50 mM potassium acetate. The dialyzed protein was diluted into three batches to final concentrations of 5.7 μM, 11.1 μM, and 19.5 μM using the final dialysis buffer. Centrifugation was at 4 °C in a Beckman Optima XLA Analytical Ultracentrifuge using 1.2-cm double sector charcoal-filled Epon centerpieces. The protein gradients were recorded at 280 nm every 2–3 h until they were superimposable. Equilibrium data were collected at 6,000, 8,400, 10,600, 13,000, and 16,000 rpm. Non-sedimenting absorbance in each sample was determined by high speed depletion at the end of the run and was <0.025 for all samples. After obtaining the equilibrium data at 16,000 rpm, the rotor was slowed to 10,600 rpm to check for reversibility. The equilibrium gradients were nearly superimposable, indicating no significant loss of protein due to irreversible aggregation at high concentrations. Absorbance in the gradients ranged from ~0 to ~1.5, which corresponds to ~0 to ~42 μM protein. The partial specific volume and molecular weight of the polypeptide were calculated from the composition as 0.743 ml/g and 33,990. The dialysate density at 4 °C was measured as 1.00351 g/ml using an Anton Paar DMA5000 density meter. The extinction coefficient used was 29800 M^{-1} cm^{-1}. The data from the three samples at five speeds were globally tested against models of a single species, two and three species in equilibrium, and two independent non-interacting species. In all models the measured non-sedimenting absorbance was included as a fixed parameter. Data analysis utilized programs developed in Igor Pro (Wavemetrics Inc., Lake Oswego, OR) by Darrell R. McCaslin.

Fluorescence Polarization Assays—RdgC protein was serially diluted in fluorescence polarization buffer. The same fluorescently labeled DNA substrates were used as in the electrophoretic mobility shift assays. The DNA was added to a final concentration of 0.7 nM molecules or 21 nM nucleotides for experiments with single-stranded oligonucleotides and 42 nM nucleotides for duplex oligonucleotides. The anisotropy of the samples was measured using a Beacon 2000 fluorescence polarization system. The data were analyzed using Curve Expert 1.37 (available at curveexpert.webhop.biz/). For challenge experiments, unlabeled DNA substrates identical to the labeled oligonucleotides were used. RdgC protein diluted in fluorescence polarization buffer was added to 0.7 nM molecules of DNA. After equilibrium binding was reached, 100-fold excess of unlabeled single-stranded or duplex oligonucleotide was added and anisotropy was monitored over time.

Electron Microscopy—A modified Alcian method was used to visualize RdgC in the presence of DNA. Activated grids were prepared as described previously (13). Samples for electron microscopy were prepared by incubating 1 μM RdgC and 4 μM M13mp8 circular ssDNA or 8 μM ϕX174 ldsDNA, 25 mM Tris-OAc (80% cation) buffer, 5% (w/v) glycerol, 3 mM potassium glutamate, and 10 mM $Mg(OAc)_2$ for 10 min.

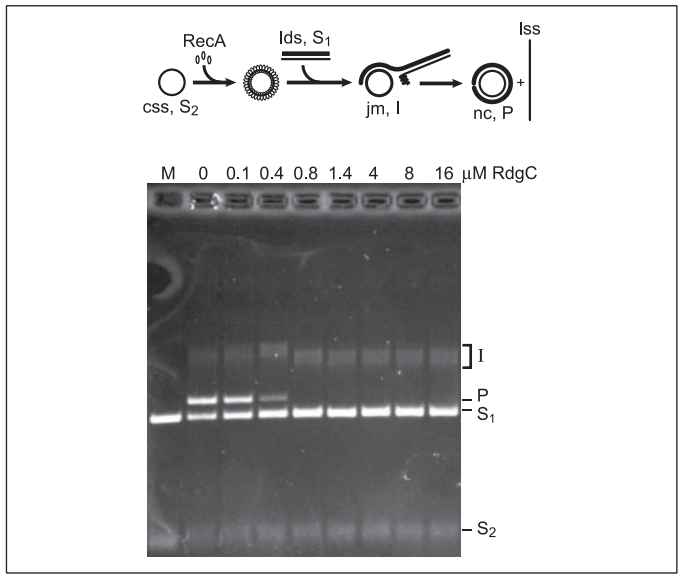

FIGURE 1. **RdgC inhibits RecA-promoted DNA strand exchange activity**. The RecA-promoted DNA strand exchange reaction is illustrated as a schematic at the *top*. The RecA protein forms a helical filament on circular single-stranded DNA (*css*, labeled *S2*) and recruits complementary linear double-stranded DNA (*lds*, labeled *S1*). RecA then pairs the two molecules, and a joint molecule (*jm*, labled *I*) is formed while the non-homologous strand is displaced. Finally, a nicked circular product (*nc*, labeled *P*) and a linear single-stranded molecule result. Substrates, products, and intermediates are distinguishable by agarose gel electrophoresis. In the experiment shown in the gel, reactions contained 3 μM RecA, 9 μM ϕX174 cssDNA and ldsDNA, 3 mM ATP, 0.9 μM SSB, and the indicated amounts of RdgC.

All incubations were at 37 °C. The reaction mixtures described above were diluted as indicated in the figure legend with 200 mM ammonium acetate, 10 mM HEPES (pH 7.5), and 10% (w/v) glycerol. The samples were prepared for analysis as described (22). To determine if RdgC-bound DNA molecules were extended or condensed relative to naked DNA, molecules were measured from micrographs magnified 52,000 or 42,000 times using the software OpenLab 3.1.7 by Improvision. Five molecules each of RdgC-bound dsDNA and naked dsDNA were measured at least three times each, and these measurements were averaged after normalization for the magnification. *Scale bars* on the micrographs were used to convert measurements into microns.

RESULTS

RdgC Protein Inhibits RecA Protein Activities—We first surveyed the effects of RdgC protein on a series of classic RecA functions. As seen in Fig. 1*B*, RdgC protein has a potent effect on RecA protein-promoted DNA strand exchange. In this series of experiments, RdgC was added after RecA filaments had formed on the ssDNA and 5 min after the ldsDNA was added. With 3 μM RecA protein present in this experiment, a sharp reduction in DNA strand exchange products was seen with 0.4 μM RdgC protein, and the generation of products was abolished at 0.8 μM RdgC. Some reaction intermediates were observed even when 16 μM RdgC was present. Additional effects of RdgC on strand exchange are described below.

The effects of RdgC on RecA-mediated ATPase activity depends on the order of addition of the proteins in a pattern suggesting a simple competition of RdgC and RecA for DNA binding sites. When RdgC protein is added after RecA filaments have formed on ssDNA, the inhibition is modest and slow to materialize (Fig. 2*A*). The concentrations of RecA and DNA are somewhat less than those in Fig. 1, yet 20 μM RdgC has little effect on activity in the first few minutes. The inhibition slowly increases with time, suggesting that RdgC is able to replace RecA protein on the DNA as RecA dissociates at filament breaks via end-depend-

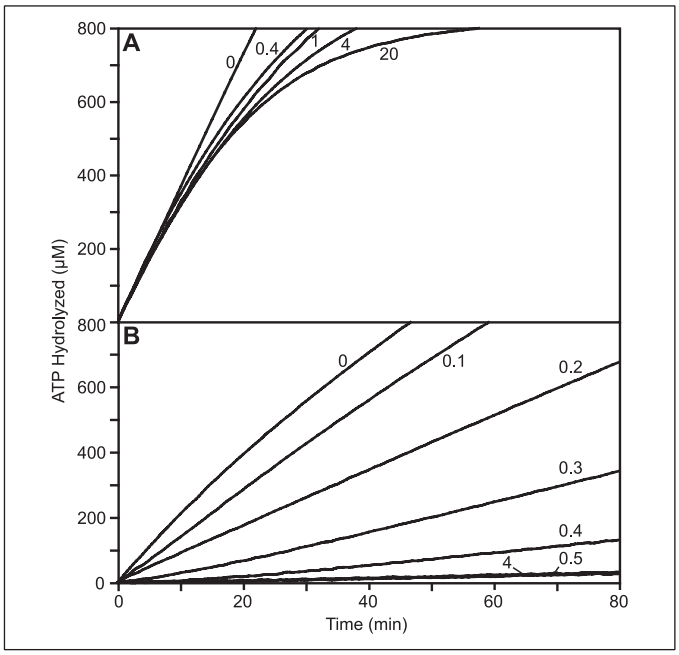

FIGURE 2. **RdgC inhibition of RecA ATPase activity reflects a competition between RecA and RdgC for DNA binding sites.** *A*, full RecA-cssDNA filaments were formed by incubating 2.4 μM RecA, 4 μM M13mp8 cssDNA, and 0.4 μM SSB before the addition of the indicated amount of RdgC protein in micromolar. *B*, reactions were conducted as in *A*, except RdgC was preincubated with cssDNA before the addition of RecA and the SSB protein was omitted. The concentrations of RdgC in micromolar are indicated in the figure.

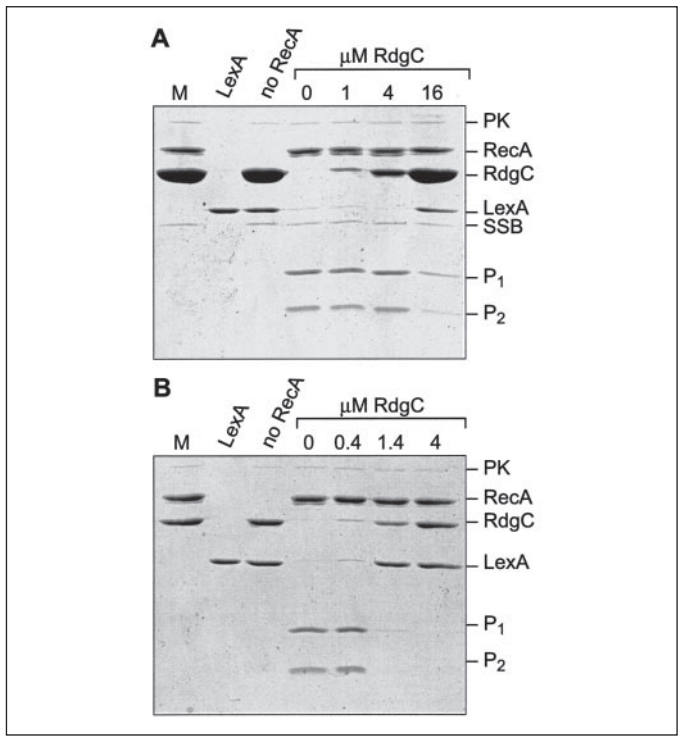

FIGURE 3. **RdgC inhibition of RecA-promoted LexA auto-cleavage also reflects a competition for DNA binding.** *A*, RecA (3 μM) was preincubated with 9 μM ϕX174 cssDNA and 0.9 μM SSB to allow full filaments to form. RdgC (concentrations indicated in micromolar) was added and incubated for 60 min before the addition of LexA (3 μM). *B*, reactions were conducted as in *A* except RdgC was preincubated with the DNA before the addition of RecA and SSB was omitted.

ent filament disassembly (23, 35). To explain the results, the RdgC binding would have to block the extension of trailing RecA filaments. Alternatively, the RdgC protein could be capping the growing ends of RecA filaments much as RecX protein appears to do (23). In the case of RdgC, the inhibition patterns are most consistent with a simple competition with RecA for DNA binding sites, as is discussed below.

When the RdgC protein was added prior to RecA protein, the RecA-mediated ATP hydrolysis declined as a direct function of RdgC protein concentration, with the effect saturating at full inhibition above 0.5 μM RdgC protein (Fig. 2*B*). We suspected that RdgC was excluding RecA from the DNA, but the effects could also reflect a direct inhibitory binding of RdgC to RecA. To determine if the RecA protein was actually free of the DNA and still active, we added excess cssDNA to the above experiment to provide substrate for any free RecA protein to bind. This produced a recovery of ATP hydrolysis to a rate equal to hydrolysis in the absence of RdgC (data not shown), indicating that RecA was free to bind the new DNA and that RdgC was not inhibiting hydrolysis directly by binding the RecA filament. It also indicates that the RdgC protein remained bound to the original DNA and is not interacting with the displaced RecA as it binds the challenge DNA. Because there is 4 μM ssDNA in the experiment shown in Fig. 2*B*, the saturation of the inhibitory effect of RdgC at 0.5 μM is consistent with a binding site size of ~8 nucleotides for RdgC, or ~16 nucleotides for an RdgC dimer. The binding of RdgC protein to M13 cssDNA appears to be sufficiently stable that RdgC is not readily displaced by RecA protein once bound (and *vice versa*). Note that sub-saturating amounts of RdgC added prior to RecA result in a steady state of RecA-mediated ATP hydrolysis, albeit at levels inversely proportional to the added RdgC concentration. This suggests that the RdgC is simply taking up space on the DNA, while RecA can bind and establish dynamic filaments on whatever free DNA is remaining. In contrast, the filament-capping activity of the RecX protein results in more complex kinetics, little indication of direct binding of RecX to DNA, and more evident effects on RecA filaments at much lower RecX concentrations (23).

A similar pattern is seen for RdgC inhibition of the LexA cleavage reaction (Fig. 3). RecA filaments bound to ssDNA promote the autocatalytic cleavage of the LexA protein (36, 37). Inhibition of LexA cleavage required high concentrations (above 4 μM) of RdgC protein and long incubation times prior to the addition of LexA when RecA protein was present before addition of RdgC (Fig. 3*A*). If RdgC protein was added first, an RdgC concentration of 1.4 μM completely blocked the access of RecA protein to the DNA and thereby inhibited LexA cleavage (Fig. 3*B*). Regardless of the order of addition, when excess RecA that was preincubated with cssDNA was added to the above reactions, LexA cleavage was restored, indicating that RdgC does not directly protect LexA (data not shown). Because even small fragments of RecA filaments on DNA are sufficient to facilitate a robust LexA cleavage reaction (23), the cessation of LexA cleavage at 1.4 μM RdgC protein (Fig. 3*B*) indicates a complete exclusion of RecA from the DNA. As indicated in earlier experiments (Fig. 2*B*), this is probably a significant excess of RdgC protein under these conditions, but one that may be necessary to eliminate even the low level of short RecA filaments needed for rapid LexA cleavage.

We were curious to discover why the effects of RdgC protein on RecA protein-promoted DNA strand exchange was so much more robust than the effects of RdgC on other RecA functions (when RdgC was added to the reaction late). One possibility is that RdgC can block DNA strand exchange, even when RecA filaments are intact, by binding to the duplex DNA substrate. In this way, the RecA nucleoprotein filaments formed on ssDNA would be relatively unaffected but would not be able to promote strand exchange with the RdgC-bound dsDNA. We tested this idea indirectly, by examining the effects of the DinI protein on

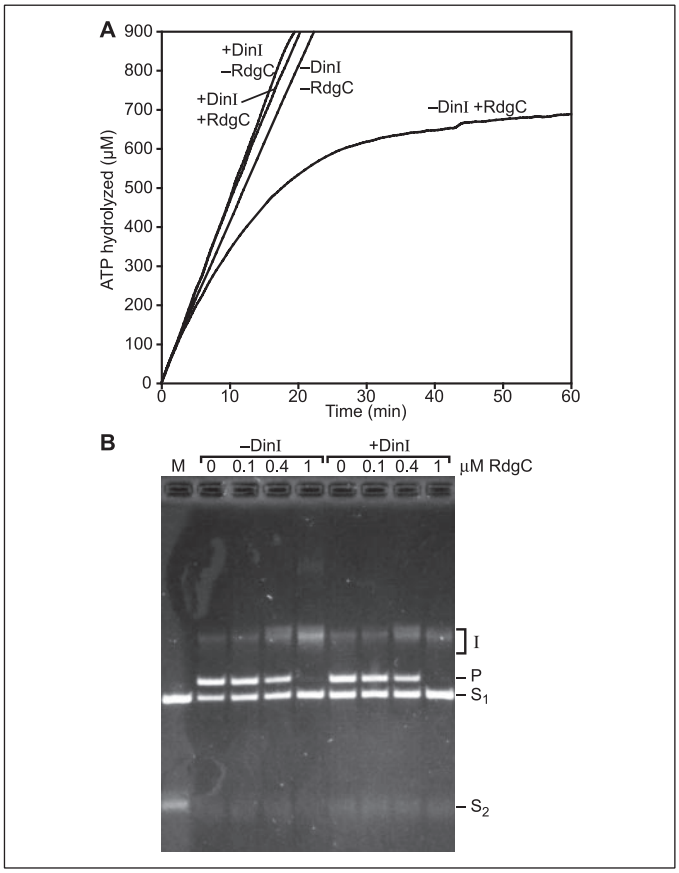

FIGURE 4. **RdgC inhibits DNA strand exchange promoted by DinI-stabilized RecA-cssDNA filaments.** *A*, reactions were conducted as in Fig. 2*A* except 16.8 μM DinI was preincubated with RecA where indicated. The concentration of RdgC is 20 μM when present. *B*, reactions were conducted as in Fig. 1, except 21 μM DinI was preincubated with RecA where indicated.

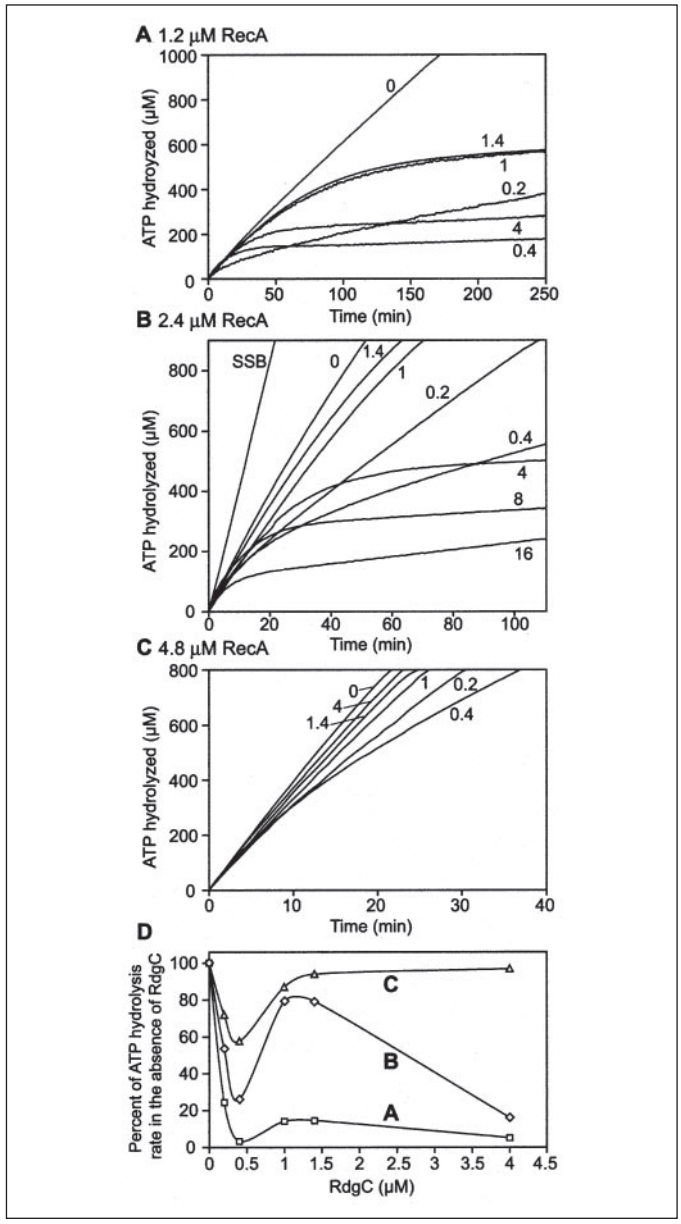

FIGURE 5. **RdgC inhibition of incomplete RecA filaments is bimodal and relates to a concentration-dependent change of state in RdgC.** RdgC (with concentrations indicated in micromolar in the figures) was titrated into reactions containing 1.2 μM RecA and 2 μM cssDNA (*A*), 2.4 μM RecA and 4 μM cssDNA (*B*), or 4.8 μM RecA and 8 μM cssDNA (*C*). The reactions did not include SSB except where noted, and RecA and cssDNA were preincubated for 6 min before the addition of RdgC. Under these conditions, RecA filaments are incomplete and DNA is exposed at the time of RdgC addition. *D*, rates of ATP hydrolysis in the presence of RdgC calculated at 170 min (*A*), 50 min (*B*), and 17 min (*C*) are plotted as percentages of the rate of hydrolysis in the absence of RdgC *versus* the concentration of RdgC.

RdgC-mediated inhibition of RecA activities. The DinI protein is known to stabilize RecA filaments (22). When DinI protein was added to RecA filaments prior to the addition of RdgC protein, the RdgC had no significant effect on RecA-mediated ATP hydrolysis (Fig. 4*A*). The same level of RdgC caused a gradual decline in ATP hydrolysis reflecting displacement of the RecA protein when DinI was not present. DinI was protective even though a rather high level of RdgC protein (20 μM) was used for the challenge. However, when DNA strand exchange was examined, RdgC protein had the same inhibitory effect regardless of whether DinI was present or not. From this we conclude that the potent effect of RdgC in the inhibition of strand exchange did not primarily reflect a displacement of RecA protein in the nucleoprotein filament by RdgC, but instead a binding of RdgC to the dsDNA substrate so as to make it unavailable to the filaments for strand exchange.

RdgC Protein Undergoes a Concentration-dependent Change in State—When RecA protein is bound to ssDNA in the absence of SSB, the resulting filaments are incomplete. Regions of secondary structure in the ssDNA impose barriers against the formation of uninterrupted RecA filaments (6, 14). Under these conditions, the inhibitory effects of RdgC are bimodal (Fig. 5*B*). Addition of RdgC at low concentrations (0.2 or 0.4 μM) triggered a decline in RecA-mediated ATP hydrolysis, suggesting that RecA protein was dissociating and being replaced by RdgC. However, when the RdgC concentration was raised to 1 μM, the effect was greatly lessened such that little inhibition was observed. A substantial inhibitory effect again asserted itself as the RdgC concentration was increased further to 4, 8, and then 16 μM. This pattern could be seen at several different concentrations of RecA protein and DNA (where RecA to DNA ratios were held constant) (Fig. 5, *A* and *C*). The amounts of RdgC required to generate maximum inhibition in the first mode were independent of RecA concentration, as were the levels of RdgC at which the inhibition was relieved (Fig. 5*D*). This indicated that the switch from inhibition to a non-inhibitory mode of action was a function of some property of the RdgC protein, rather than RecA or a complex of RecA and RdgC. The observed decline in the inhibitory effects suggests that RdgC protein is somehow being withdrawn from the reaction. We suggest later that this may reflect the sequestering of RdgC into an inactive aggregate or oligomer.

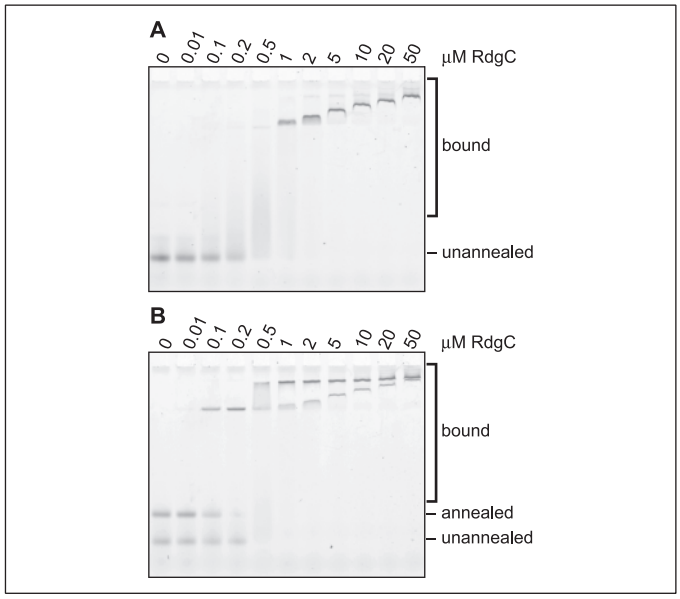

FIGURE 6. **RdgC aggregates/oligomerizes as it binds DNA.** Reactions contained 10 nM (molecules) fluorescently labeled 30 nucleotide single-stranded DNA (*A* and *B*), 30-bp duplex oligonucleotide (*B*) and the indicated amount of RdgC protein in micromolar. An electrophoretic mobility shift assay was used to assess binding.

An apparent oligomerization can be seen in the patterns of RdgC protein binding to short oligonucleotides. As RdgC binds to a 30-bp single-stranded oligonucleotide, a complex is readily seen at RdgC concentrations above 0.2 μM (Fig. 6*A*). As more RdgC protein is added, the migration of the RdgC-DNA complex is progressively impeded as though more and more RdgC protein was being added to it. No single discrete RdgC-ssDNA complex is evident. When the RdgC protein was added to a mixture of ssDNA and dsDNA oligonucleotides, a discrete RdgC-dsDNA complex was observed at lower RdgC concentrations (0.1–0.5 μM) (Fig. 6*B*). At higher RdgC concentrations this again gives way to slower migrating species that could be RdgC-DNA aggregates. The results suggest that RdgC may be in equilibrium between two or more forms that differ in competitiveness with RecA protein for binding to ssDNA and dsDNA. Formation of higher molecular weight species may not occur unless a critical concentration of RdgC protein is present.

RdgC Protein Exists as a Mixture of Oligomers in Equilibrium—To directly determine the oligomeric state of RdgC, we performed sedimentation equilibrium experiments. When plotted as the logarithm of absorbance *versus* squared radial position, the equilibrium data for RdgC was curved to varying degrees depending on speed and initial concentration, which requires the presence of more than a single molecular weight species. The inability of a homogeneous single dimeric species to describe the data is illustrated in Fig. 7*A*. Analysis of the log plots indicated the presence of monomeric RdgC and species larger than a dimer. Various models with equilibria between the monomer and one or two higher oligomers were fit globally to the complete data set. Of the two species models, a monomer-trimer equilibrium was the best fit, and gave a molecular weight 1.2 times the polypeptide weight and an aggregation number of 3.0. Fixing the molecular weight at the polypeptide weight increased the aggregation number to 3.2 but had little effect on the overall quality of the fit. Fixing both the molecular weight and the aggregation number increases the fit variance slightly, and the fit residuals become slightly less random. A monomer-dimer-trimer model required a negative equilibrium constant for dimerization and is rejected on that basis. A model with a monomer-dimer-tetramer equilibrium fit approximately as well as the monomer-trimer model. The molecular weight from the global fit was 0.91 times the polypeptide weight with relative errors in the fitted equilibrium constants of 7 and 11%. Fixing the molecular weight to that of the polypeptide did not alter the quality of the fits and resulted in relative errors in both equilibrium constants of ~5%. The fit to the monomer-dimer-tetramer model for the 13000 rpm data is shown in Fig. 7*A*. Although the data do not permit a definitive choice between the monomer-trimer and the monomer-dimer-tetramer model, the latter is more consistent with previous data that indicate the presence of a dimer. Gel filtration of RdgC conducted by ourselves (data not shown) and Moore *et al.* (26) suggested a 70-kDa species, which corresponds to a dimer. A glutaraldehyde cross-linking study also by Moore *et al.* (26) could not distinguish between a dimer and a trimer; however, because there were no intermediate species, the authors decided it was most likely a dimer. Finally, atomic force microscopy of RdgC protein conducted by Tessmer *et al.* (38) reveals complexes with volumes that correspond to monomers, dimers, and an undetermined higher order species that could be a tetramer. The presence of different oligomeric species of RdgC in solution helps explain the different modes of inhibition of RecA. It is possible that the monomer and tetramer are both inhibitory species. At low concentrations of RdgC, the protein exists almost exclusively as monomers (Fig. 7*B*). The proportion of species shifts to more and more dimers as the concentration of RdgC increases. Perhaps RecA is more capable of displacing dimers of RdgC from the DNA, leading to the decrease in inhibition seen in Fig. 5. Tetramers begin to form at yet higher concentrations of RdgC, starting at around 2 μM (Fig. 7*B*). Because the inhibition seen in Fig. 5 is restored when there is still a proportionally small amount of tetramers, they may be the species with the most potent inhibitory effect, possibly by having a higher affinity for DNA.

RdgC Protein Has a High Affinity for dsDNA, and Binding to DNA Is Bimodal—Because RdgC binding to DNA appears to be central to the mechanism of inhibition of RecA, we used a second method to investigate RdgC-DNA binding, fluorescence polarization. The same fluorescently labeled single-stranded and duplex 30-mer oligonucleotide substrates were used as in the electrophoretic mobility shift assays. As is evident in Fig. 8*A*, RdgC binding to duplex DNA is bimodal. This supports the idea that different oligomeric species of RdgC behave differently. Perhaps monomers of RdgC, present in the highest proportion at low concentrations, are responsible for the first binding curve while higher order complexes of RdgC at higher concentrations lead to the second curve (Fig. 8*A*).

We then conducted challenge experiments. RdgC (at 30 nM or 50 nM for ss- and dsDNA, respectively) was added to the fluorescently labeled DNA, and anisotropy was monitored over time (Fig. 8*B*). After equilibrium was reached, a 100-fold excess of unlabeled DNA was added to challenge the RdgC-DNA complexes. As seen in Fig. 8*B*, challenging RdgC bound to ssDNA with unlabeled dsDNA results in a large decrease in anisotropy, indicating that the dsDNA competes well with the ssDNA for RdgC binding. This suggests that RdgC has a higher affinity for duplex DNA. The converse experiment also supports this conclusion. Challenging RdgC bound to dsDNA with excess ssDNA leads to only a small decrease in anisotropy. A previous study of RdgC-DNA binding also concluded that RdgC has a higher affinity for dsDNA (26). The capacity of excess dsDNA to disrupt RdgC-dsDNA complexes (Fig. 8*B*) may indicate that there is more than one binding site for dsDNA on an RdgC dimer.

Visual inspection of RdgC in the presence of DNA by electron microscopy supports the idea that RdgC preferentially binds dsDNA. On ϕX174 ldsDNA (5386 bp), RdgC can be seen uniformly coating the full length of the DNA (Fig. 9*A*). Of 226 molecules counted, 100%

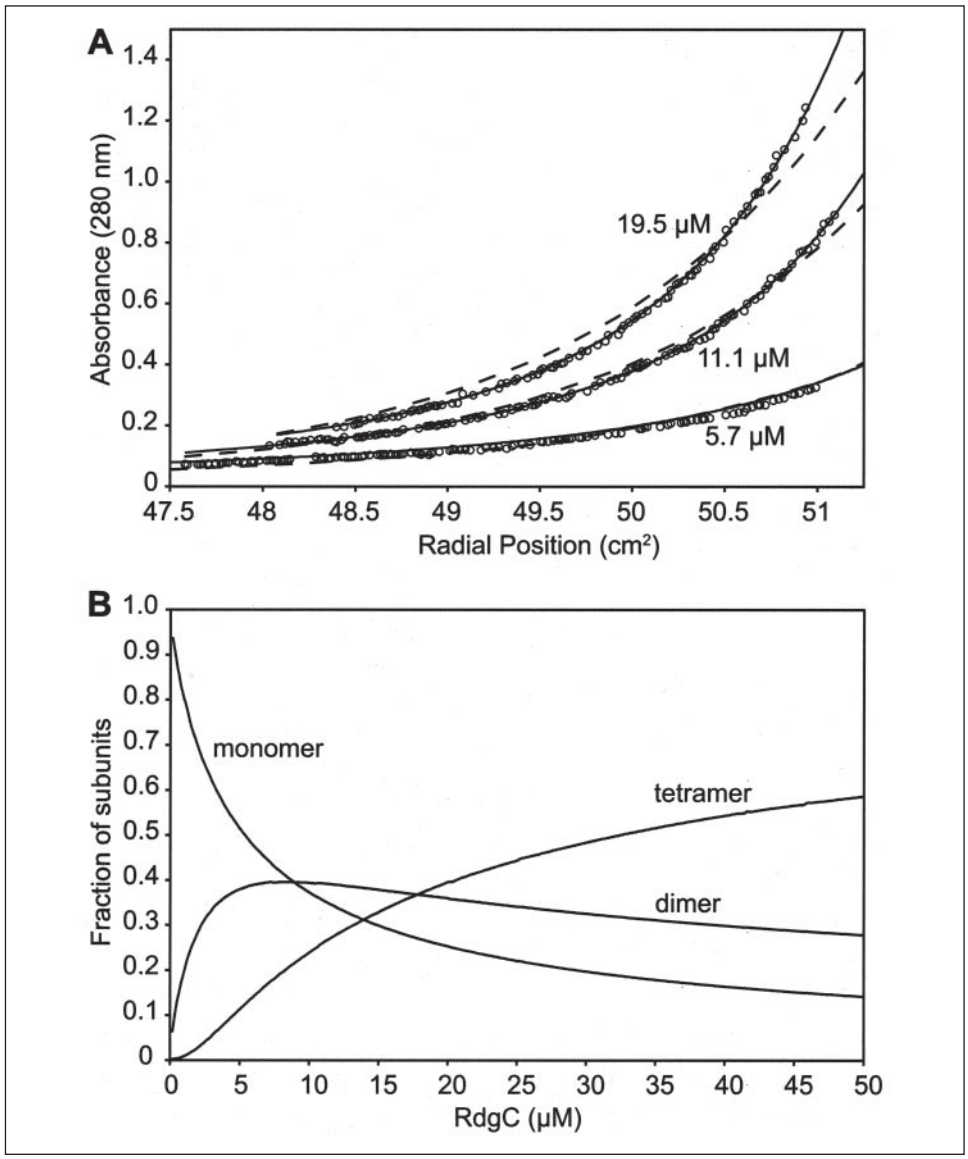

FIGURE 7. **RdgC exists not as a single species but as a mixture of oligomers in equilibrium.** *A*, a monomer-dimer-tetramer model (*solid lines*) fits the data (*open circles*) much better than a model for just dimers (*dashed lines*). The data are from three concentrations of RdgC (figure labels) at 13000 rpm. *B*, the fraction of subunits present as monomers, dimers, and tetramers is plotted *versus* the concentration of RdgC protein.

appeared to be fully protein-coated under these conditions, which include excess RdgC protein. The general appearance of these molecules was uniform, and all followed the form illustrated in Fig. 9*A*. A small sample (5) of these RdgC-coated dsDNA molecules, chosen at random, was measured as described under "Experimental Procedures." The same number of unbound dsDNA molecules was similarly measured. Within experimental error, the lengths of each of the five molecules measured in a sample were identical. The maximum error between measurements of an individual molecule was 0.029 μm. The average length of the bound DNA molecules was 1.992 $\pm$ 0.103 μm compared with 1.968 $\pm$ 0.079 μm for the unbound DNA, which is again identical within experimental error (the error given is $\pm$ one S.D.). This indicates that the DNA was neither extended nor condensed when bound by RdgC protein. The RdgC protein can also be seen binding M13mp8 cssDNA (7229 nucleotides). In this case, it appears that the protein-coated DNA molecule is highly condensed and folded (Fig. 9*B*). Essentially all molecules on the grid had a similar condensed structure. The branched appearance of the molecules could reflect regions of secondary structure where RdgC is bound to duplex regions in the DNA. Electron micrographs of the RecA protein bound to M13 cssDNA give a much different appearance. As would be expected for a protein that preferentially binds ssDNA, these micrographs show extended circles of protein-coated DNA with no evidence of branching (39–41). In the absence of bound protein, the cssDNA substrate is almost impossible to visualize when prepared using the Alcian method, and we did not observe unbound DNA in this control carried out side by side with the experiments with RdgC-bound cssDNA shown in Fig. 9*B*. This indicates that the aggregates visualized in Fig. 9*B* are RdgC protein-dependent.

A higher affinity for regions of secondary structure in ssDNA could explain the potent inhibition that RdgC has on RecA protein-mediated ATP hydrolysis when RdgC is pre-bound to M13 cssDNA (Fig. 2*B*). In contrast, much greater concentrations of RdgC are necessary to inhibit RecA ATP hydrolysis on poly(dT) (Fig. 10*A*). Unlike M13 DNA, poly(dT) ssDNA has no secondary structure. A lower affinity of RdgC for ssDNA could allow RecA to compete better for DNA binding sites on poly(dT), whereas RdgC can bind to the duplex regions of secondary structure of M13 and prevent extension and melting by RecA. At relatively high concentrations of RdgC (4 μM) on poly(dT), it appears that RecA is able to displace RdgC and recover ATPase activity (Fig. 10*A*), supporting the idea that RdgC binds weakly to ssDNA. More RdgC is also required to inhibit RecA when RecA is pre-bound to poly(dT), as

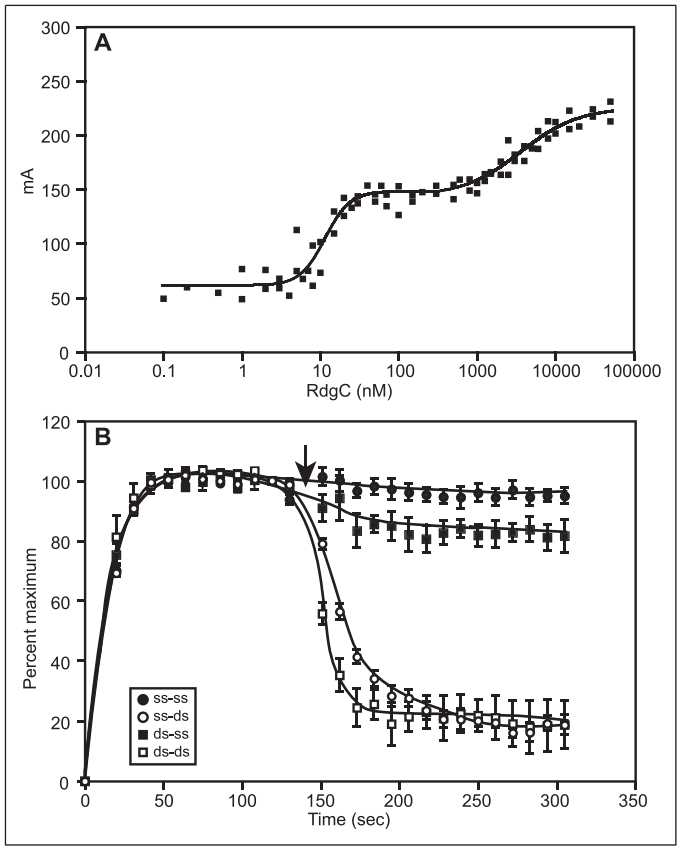

FIGURE 8. **RdgC binding to DNA.** *A*, anisotropy increases in a bimodal pattern as RdgC binds to duplex 30-mer fluorescently labeled DNA oligonucleotides. Units (mA) are millianisotropy units. The data from two independent experiments are plotted. *B*, challenge experiments. RdgC pre-bound to fluorescently labeled DNA substrates was challenged with a 100-fold excess of unlabeled DNA. Anisotropy units were normalized as a percentage of maximum signal and plotted *versus* time. Each point is the average of three trials, and *error bars* represent one standard error. An *arrow* indicates the time that excess unlabeled DNA was added.

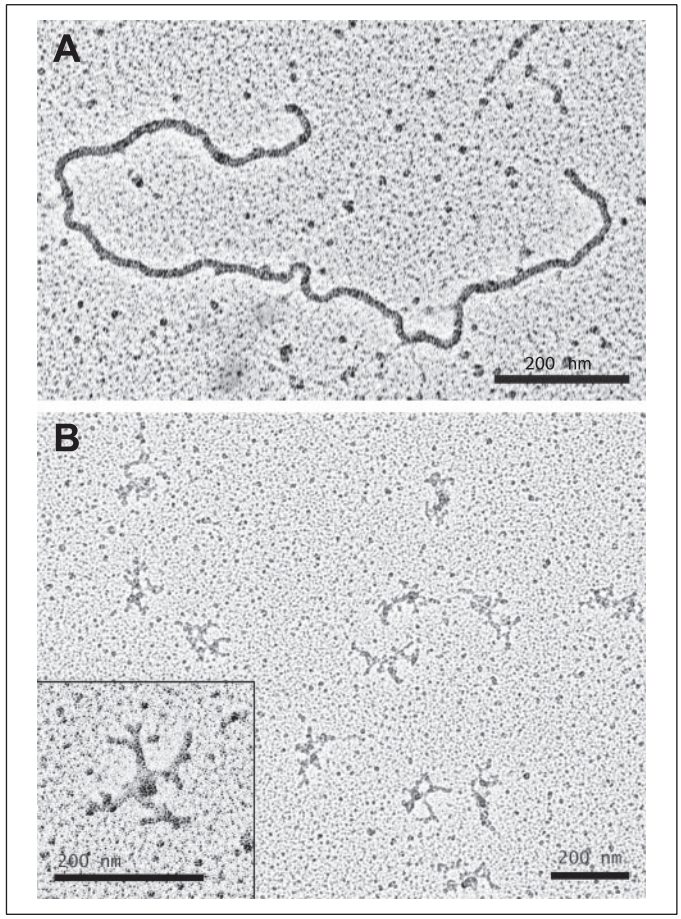

FIGURE 9. **Electron microscopy of RdgC-DNA complexes.** RdgC (1 μM) was incubated with 8 μM ϕX174 ldsDNA (*A*) or 4 μM M13 cssDNA (*B*) for 10 min at 37 °C before being diluted 6.6-fold (*A*) or 3.3-fold (*B*) and adhered to electron microscopy grids.

compared with the same order of addition when using the M13 ssDNA (Figs. 10*B* and 5*B*).

RdgC and SSB Proteins Inhibit RecA Filament Formation Additively—The SSB protein inhibits RecA filament nucleation when it is bound to ssDNA prior to RecA. However, the same SSB will facilitate RecA filament extension by eliminating regions of secondary structure in the DNA (42, 43). RecA displaces SSB readily during the extension phase but not during nucleation. Subsaturating levels of SSB thus allow nucleation and facilitate RecA filament extension, leading to an overall improvement in the levels of bound RecA (Fig. 11). Higher SSB levels produce a long lag in RecA binding. When RdgC protein is also present on the DNA, the lag in RecA binding is converted to a more or less permanent exclusion from the DNA. An addition of 0.3 μM RdgC, enough to occupy somewhat more than half the ssDNA present, largely suppresses the establishment of RecA filaments in the presence of 0.4 μM SSB (Fig. 11).

Deletion of the RecA C Terminus Reduces the Effects of RdgC Protein—Removal of the 17 C-terminal amino acids of RecA protein results in a truncated protein with more robust recombinase functions (12–14). The RecAΔC17 mutant binds more rapidly to duplex DNA, rapidly displaces SSB from ssDNA during the nucleation phase of filament formation, and promotes DNA strand exchange without the need to add excess free Mg^{2+} ion to the reaction buffer (12–14). When RdgC protein is added to filaments of RecAΔC17 protein formed on ssDNA, there is little effect seen in the rates of ATP hydrolysis mediated by the mutant RecA (Fig. 12*A*). Under the same conditions, the wild-type RecA protein is slowly replaced by RdgC (Fig. 12*A*). The result suggests that the mutant protein simply does not dissociate and thus does not afford an opportunity for RdgC binding.

The situation is quite different on dsDNA. The more rapid binding of RecAΔC17 to dsDNA provides an opportunity to examine the competition between RdgC and RecA (at least in mutant form) on this substrate. In the absence of RdgC, RecAΔC17 protein binds to the dsDNA with a lag time of ~15 min (Fig. 12*B*). If the filaments are challenged by addition of RdgC, the rate of ATP hydrolysis drops off abruptly and dramatically. The drop off is much faster than would be anticipated from normal end-dependent disassembly from RecA filaments ends (44) and here suggests an active displacement of RecAΔC17 from the DNA by RdgC protein. An alternative explanation would be a suppression of RecAΔC17-mediated ATP hydrolysis by complex formation with RdgC, without displacement of the mutant RecA protein. If circular ssDNA is subsequently added to the reaction, the rates of ATP hydrolysis rapidly recover to those expected for RecAΔC17 bound to ssDNA. This indicates that the RecAΔC17 protein has indeed been displaced by RdgC and is available for binding to the ssDNA (Fig. 12*B*). The results indicate that RdgC competes with RecAΔC17 protein much more effectively on dsDNA than on ssDNA.

DISCUSSION

We conclude that RdgC protein interferes with RecA function primarily by competing with it for DNA binding sites. If RecA protein

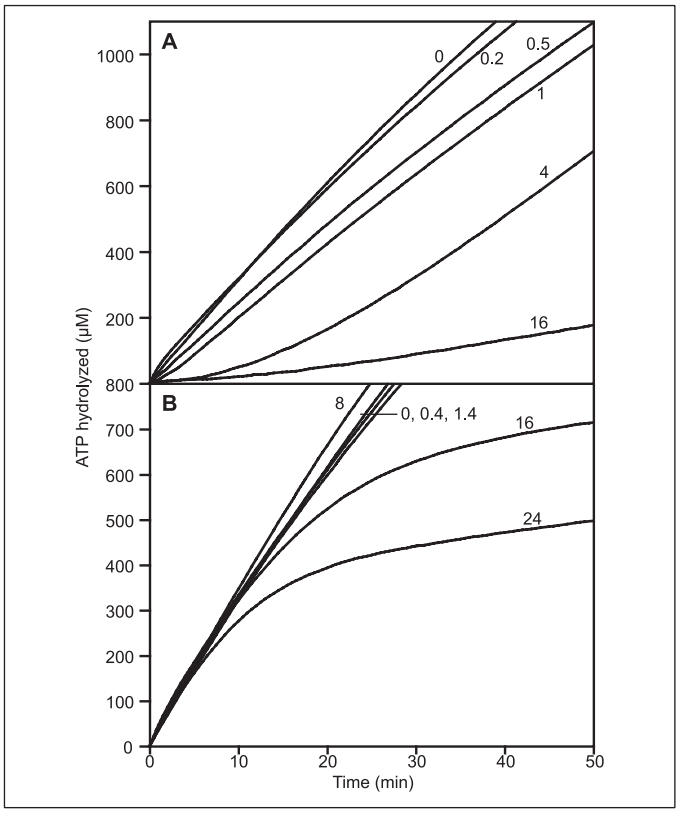

FIGURE 10. **RecA competes better with RdgC on poly(dT) than it does on M13 cssDNA.** Reactions contained 2. 4 μM RecA, 4 μM poly(dT), and the indicated amount of RdgC in micromolar. *A*, RdgC was preincubated with the DNA for 5 min before RecA was added. *B*, RecA was preincubated with the DNA for 6 min before RdgC was added. Compare with Figs. 2*B* and 5*B*.

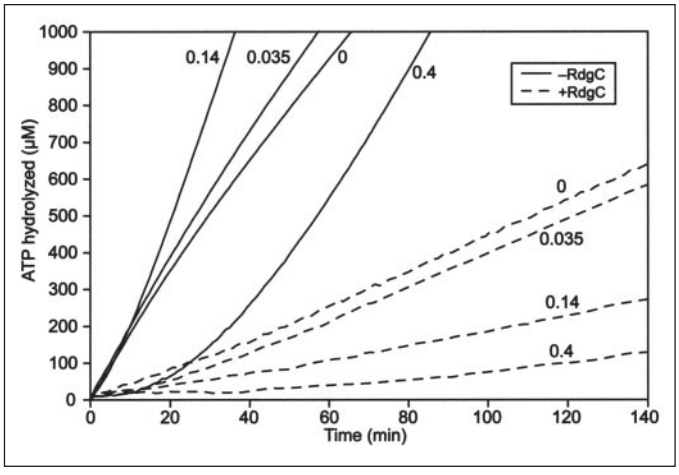

FIGURE 11. **The RdgC and SSB proteins inhibit RecA synergistically.** Reactions were conducted as in Fig. 2*A* except that RdgC and SSB were preincubated with the cssDNA before the addition of RecA. Reactions contained 0.3 μM RdgC where indicated and concentrations of SSB that were saturating (0.4 μM) and subsaturating (0.14 and 0.035 μM) for the amount of DNA present (4 μM).

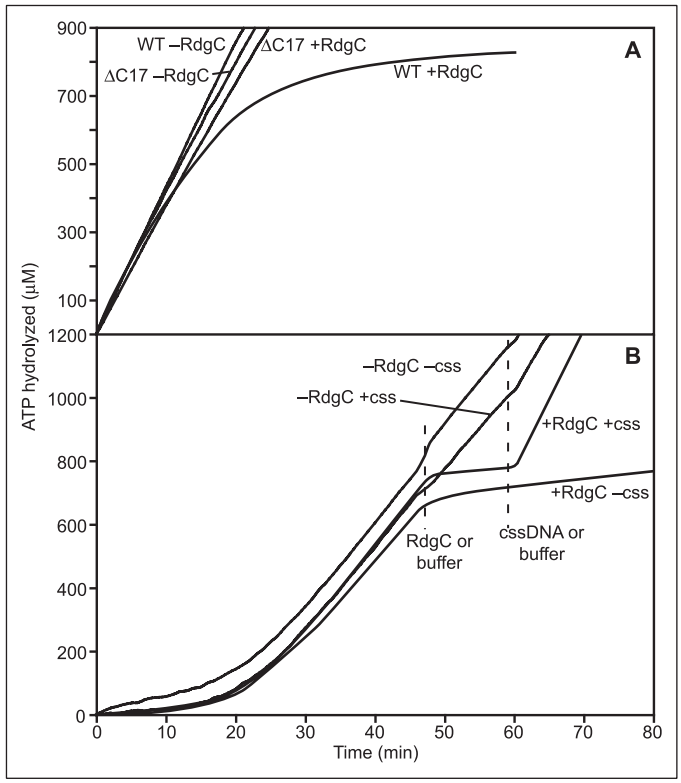

FIGURE 12. **RdgC inhibition of the RecAΔC17 mutant.** *A*, reactions were conducted as in Fig. 2*A* and contain 2.4 μM WT RecA or RecAΔC17 and 20 μM RdgC, where indicated. *B*, RecAΔC17 (2.4 μM) was preincubated with ϕX174 ldsDNA before the addition of either 1 μM RdgC or buffer when indicated, followed by a second addition of either cssDNA or buffer.

filaments are bound to ssDNA, RdgC protein has little effect on the function of those filaments except to replace any RecA that should dissociate. If RdgC protein is bound to the ssDNA first, it is effective in excluding RecA from the DNA, especially if the ssDNA has some duplex character due to secondary structure. The competition is even more evident on dsDNA. Here, RdgC binds better and appears to displace even pre-formed filaments of RecAΔC17 protein. The apparently tight binding of RdgC protein to dsDNA has the additional effect of sequestering the dsDNA substrate and denying it to otherwise active RecA nucleoprotein filaments for use in DNA strand exchange.

RdgC protein is a DNA-binding protein that has been implicated in some indirect roles in recombinational DNA repair and other recombinational processes (26, 45). RdgC may have a role in preventing the inappropriate formation of RecA filaments in some situations (26). It is clear from the present results that RdgC is effective at preventing RecA binding to DNA. On a ssDNA substrate, RdgC is much more effective than SSB in restricting access of RecA to the DNA. To the extent that RecA function is impaired, it is impaired indirectly as a result of RdgC-mediated exclusion from DNA binding sites, especially dsDNA binding sites. It could be that RdgC plays a role in restricting RecA binding to ssDNA gaps, where RecA functions are most useful to the cell. There is little evidence for a direct interaction between RdgC and RecA. The one case where interaction may occur involves the observed competition on dsDNA, where the rapid removal of RecAΔC17 protein from the DNA may reflect an active displacement by RdgC protein.

RdgC clearly has the capacity to interfere with RecA reactions, and the present work establishes a baseline for that interference. However, if there is no clear interaction between RdgC and RecA, how would the RdgC be targeted to sites of RecA activity? The answer may involve an interaction between RdgC protein and one or more of the other proteins that modulate RecA function. We note that the deleterious effects of an *rdgC* deletion in certain mutant backgrounds are suppressed by mutations in the *recF*, *recO*, *recR*, or *ssb* genes (26). In principle, RdgC protein could interfere with RecA function by interacting with any of the protein products of these genes, and this is the avenue that now needs exploration.

Acknowledgments—We thank Elizabeth Wood for cloning the rdgC gene and expressing the native RdgC protein, and Shelley Lusetti for purifying the RdgC protein.

REFERENCES

1. Cox, M. M., Goodman, M. F., Kreuzer, K. N., Sherratt, D. J., Sandler, S. J., and Marians, K. J. (2000) *Nature* **404,** 37–41
2. Cox, M. M. (2001) *Proc. Natl. Acad. Sci. U. S. A.* **98,** 8173–8180
3. Cox, M. M. (2002) *Mutat. Res.* **510,** 107–120
4. Kowalczykowski, S. C. (2000) *Trends Biochem. Sci.* **25,** 156–165
5. Kuzminov, A. (1999) *Microbiol. Mol. Biol. Rev.* **63,** 751–813
6. Lusetti, S. L., and Cox, M. M. (2002) *Annu. Rev. Biochem.* **71,** 71–100
7. Bork, J. M., Cox, M. M., and Inman, R. B. (2001) *J. Biol. Chem.* **276,** 45740–45743
8. Shan, Q., Bork, J. M., Webb, B. L., Inman, R. B., and Cox, M. M. (1997) *J. Mol. Biol.* **265,** 519–540
9. Register, J. C., III, and Griffith, J. (1985) *J. Biol. Chem.* **260,** 12308–12312
10. Lindsley, J. E., and Cox, M. M. (1990) *J. Biol. Chem.* **265,** 9043–9054
11. Yu, V. P., Koehler, M., Steinlein, C., Schmid, M., Hanakahi, L. A., van Gool, A. J., West, S. C., and Venkitaraman, A. R. (2000) *Genes Dev.* **14,** 1400–1406
12. Lusetti, S. L., Shaw, J. J., and Cox, M. M. (2003) *J. Biol. Chem.* **278,** 16381–16388
13. Lusetti, S. L., Wood, E. A., Fleming, C. D., Modica, M. J., Korth, J., Abbott, L., Dwyer, D. W., Roca, A. I., Inman, R. B., and Cox, M. M. (2003) *J. Biol. Chem.* **278,** 16372–16380
14. Eggler, A. L., Lusetti, S. L., and Cox, M. M. (2003) *J. Biol. Chem.* **278,** 16389–16396
15. Umezu, K., and Kolodner, R. D. (1994) *J. Biol. Chem.* **269,** 30005–30013
16. Webb, B. L., Cox, M. M., and Inman, R. B. (1997) *Cell* **91,** 347–356
17. Morimatsu, K., and Kowalczykowski, S. C. (2003) *Mol. Cell* **11,** 1337–1347
18. Voloshin, O. N., Ramirez, B. E., Bax, A., and Camerini-Otero, R. D. (2001) *Genes Devel.* **15,** 415–427
19. Yasuda, T., Morimatsu, K., Horii, T., Nagata, T., and Ohmori, H. (1998) *EMBO J.* **17,** 3207–3216
20. Yasuda, T., Morimatsu, K., Kato, R., Usukura, J., Takahashi, M., and Ohmori, H. (2001) *EMBO J.* **20,** 1192–1202
21. Yoshimasu, M., Aihara, H., Ito, Y., Rajesh, S., Ishibe, S., Mikawa, T., Yokoyama, S., and Shibata, T. (2003) *Nucleic Acids Res.* **31,** 1735–1743
22. Lusetti, S. L., Voloshin, O. N., Inman, R. B., Camerini-Otero, R. D., and Cox, M. M. (2004) *J. Biol. Chem.* **279,** 30037–30046
23. Drees, J. C., Lusetti, S. L., Chitteni-Pattu, S., Inman, R. B., and Cox, M. M. (2004) *Mol. Cell* **15,** 789–798
24. Drees, J. C., Lusetti, S. L., and Cox, M. M. (2004) *J. Biol. Chem.* **279,** 52991–52997
25. Stohl, E. A., Brockman, J. P., Burkle, K. L., Morimatsu, K., Kowalczykowski, S. C., and Siefert, H. S. (2003) *J. Biol. Chem.* **278,** 2278–2285
26. Moore, T., McGlynn, P., Ngo, H. P., Sharples, G. J., and Lloyd, R. G. (2003) *EMBO J.* **22,** 735–745
27. Ryder, L., Sharples, G. J., and Lloyd, R. G. (1996) *Genetics* **143,** 1101–1114
28. Craig, N. L., and Roberts, J. W. (1981) *J. Biol. Chem.* **256,** 8039–8044
29. Shan, Q., Cox, M. M., and Inman, R. B. (1996) *J. Biol. Chem.* **271,** 5712–5724
30. Lohman, T. M., and Overman, L. B. (1985) *J. Biol. Chem.* **260,** 3594–3603
31. Lovett, S. T., and Kolodner, R. D. (1989) *Proc. Natl. Acad. Sci. U. S. A.* **86,** 2627–2631
32. Marrione, P. E., and Cox, M. M. (1995) *Biochemistry* **34,** 9809–9818
33. Neuendorf, S. K., and Cox, M. M. (1986) *J. Biol. Chem.* **261,** 8276–8282
34. Morrical, S. W., Lee, J., and Cox, M. M. (1986) *Biochemistry* **25,** 1482–1494
35. Arenson, T. A., Tsodikov, O. V., and Cox, M. M. (1999) *J. Mol. Biol.* **288,** 391–401
36. Little, J. W. (1991) *Biochimie* (*Paris*) **73,** 411–422
37. Kim, B., and Little, J. W. (1993) *Cell* **73,** 1165–1173
38. Tessmer, I., Moore, T., Lloyd, R. G., Wilson, A., Erie, D. A., Allen, S., and Tendler, S. J. (2005) *J. Mol. Biol.* **350,** 254–262
39. Howard-Flanders, P., West, S. C., Cassuto, E., Hahn, T., Egelman, E., and Stasiak, A. (1987) in *DNA Replication and Recombination* (McMacken, R., and Kelly, T. J., eds) pp. 609–617, Alan R. Liss, New York
40. Yu, X., and Egelman, E. H. (1992) *J. Mol. Biol.* **227,** 334–346
41. Ogawa, T., Yu, X., Shinohara, A., and Egelman, E. H. (1993) *Science* **259,** 1896–1899
42. Kowalczykowski, S. C., and Krupp, R. A. (1987) *J. Mol. Biol.* **193,** 97–113
43. Alani, E., Thresher, R., Griffith, J. D., and Kolodner, R. D. (1992) *J. Mol. Biol.* **227,** 54–71
44. Cox, J. M., Tsodikov, O. V., and Cox, M. M. (2005) *PLoS Biol.* **3,** 231–243
45. Moore, T., Sharples, G. J., and Lloyd, R. G. (2004) *J. Bacteriol.* **186,** 870–874